Electronic Supplementary Information

Enhanced oxygen reduction reaction performance of size-controlled Pt nanoparticles on polypyrrole-functionalized carbon nanotubes

Kentaro Ichihashi,[a] Satoshi Muratsugu,*[a] Shota Miyamoto,[a] Kana Sakamoto,[a] Nozomu Ishiguro,[b] and Mizuki Tada*[a, b, c]

[a] Department of Chemistry, Graduate School of Science, Nagoya University, Furo-cho, Chikusa-ku, Nagoya, Aichi 464-8602, Japan

[b] Element Visualization Team, Materials Visualization Photon Science Group, RIKEN SPring-8 Center, 1-1-1 Koto, Sayo, Hyogo 679-5198, Japan

[c] Research Center for Materials Science (RCMS) & Integrated Research Consortium on Chemical Science (IRCCS), Nagoya University, Furo-cho, Chikusa-ku, Nagoya, Aichi 464-8602, Japan

Experimental Section

Synthesis of complex 1

All chemicals were purchased from commercial sources (Wako Chemicals, Kishida Chemicals, and Sigma-Aldrich) and used without further purification unless noted. $Pt_4(\mu\text{-}OCOCH_3)_8$ was synthesized according to a literature procedure.[1]

A solution of pyrrole-3-carboxylic acid (0.27 g, 2.4 mmol) in dry acetone (15 mL) was added to a solution of $Pt_4(\mu\text{-}OCOCH_3)_8$ (0.30 g, 0.24 mmol) in dry acetonitrile (24 mL) under an N_2 atmosphere. The reaction mixture was stirred, and then the solvent was evacuated. Dry acetone (10 mL) and acetonitrile (10 mL) were added to the solid and stirred to form a suspension, and the solvent was evacuated again. This procedure was repeated 16 times. The solid was triturated with diethyl ether (50 mL) in an ultrasonic bath (40 kHz) and filtered. The precipitate was washed with a small amount of chloroform and filtered. The precipitate was dissolved in acetone, filtered again, and the filtrate was concentrated by a rotary evaporator. The ocher precipitate of **1** was collected and dried in vacuo for 12 h. Yield: 91%. ^{1}H NMR (600 MHz, DMF-d_7, ppm): δ = 11.4 (s, 4H; NH), 7.66 (dd, J = 4.8, 2.0 Hz, 4H; pyrrole-H), 6.92 (dd, J = 4.1, 2.7 Hz, 4H; pyrrole-H), 6.72 (dd, J = 2.8, 1.4 Hz, 4H; pyrrole-H), 2.02 (s, 12H; CH_3). ^{13}C NMR (150 MHz, DMF-d_7, ppm): δ = 194.2 (CH_3*C*OO), 180.1 (C_4H_4N-*C*OO), 124.8 (pyrrole-C), 119.5 (pyrrole-C), 116.7 (pyrrole-C), 110.2 (pyrrole-C), 21.10 (*C*H_3COO). Elemental analysis calcd. for $C_{28}H_{28}N_4O_{16}Pt_4 \cdot C_3H_6O$: C: 24.6, H: 2.26, N: 3.70. Found: C: 25.1, H: 2.44, N: 3.39. ESI-TOF-MS (CH_3CN): *m/z* 1479.0527 $[M + Na]^+$ (calcd. for $C_{28}H_{28}N_4O_{16}Pt_4Na$, 1478.9971), 1495.0281 $[M + K]^+$ (calcd. for $C_{28}H_{28}N_4O_{16}Pt_4K$, 1494.9709).

Characterization of complex 1

The ^{1}H, ^{13}C NMR, ^{1}H-^{1}H COSY, HMQC, and HMBC spectra of **1** were measured using an NMR spectrometer (ECA600, JEOL) at 293 K. ESI-TOF-MS spectra of **1** (Fig. I) were measured using a mass spectrometer (LCT PremierXE, Waters). Elemental analysis of **1** was conducted using an elemental analyzer (CHN Corder MT-6, Yanako).

Preparation of A-noPPy (without polypyrrole matrix overlayers)

A suspension of MWCNTs (0.10 g) in acetone (50 mL) was treated in an ultrasonic water bath (40 kHz) for 2 h at 283 K, and then the suspension was cooled to 274.5 K for 0.5 h with stirring. A solution of **1** (46.9 mg, 2.89 μmol; maximum Pt loading was estimated to be 20 wt%) in acetone (20 mL) was added to this suspension with stirring, and the mixture was stirred for 3 h at 274.5 K. The solvent was removed under reduced pressure while the system was sonicated in an ultrasonic bath (40 kHz) for 0.5 h at 283 K. The solid was dried in vacuo at 333 K for 12 h, and then placed in a glass flow cell, which was attached to a vacuum line. After evacuating the cell (ca. 10^{-2} Pa), the solid was heated to 573 K for 1 h and held at that temperature for 1 h. H_2 (99.9999%, 40 kPa) was passed through the cell for 1 h at 573 K to obtain **A-noPPy**. The actual Pt loading was estimated by X-ray fluorescence (XRF).

Characterization

XRF: XRF was measured using an XRF spectrometer (JSX-1000S, JEOL). The Pt loading was estimated from the Pt/Si peak intensity ratio by mixing the sample with the same amount of SiO_2 (Aerosil 200, Nippon Aerosil Co., Ltd.) and measuring the CPS intensities of Pt L_α and Si K_α characteristic X-rays. Samples for the calibration curves were prepared as follows. An equivalent amount of MWCNTs and SiO_2 were mixed and the mixture was impregnated with platinum acetylacetonate (Wako Chemicals) by using acetone (Wako Chemicals). The XRF samples were prepared as follows. An equivalent amount of the sample and SiO_2 were ground well with a mortar and pestle, and the mixture (20 mg) was pressed (2 MPa) into a pellet disk. For the calibration curves, disk samples (20 mg) were prepared in a similar manner.

BET analysis: Nitrogen adsorption was performed on a sorption analyzer (Micromeritics ASAP-2020, Shimadzu) at 77 K. Each sample (150 mg) was degassed at 423 K for 2 h before the adsorption measurement, and the dead volume was estimated by using pure He (99.9999%).

Thermogravimetric analysis: Thermogravimetric analysis (TGA) was performed using a thermogravimetric analyzer (TGA550, TA instruments). For the TGA measurements, the sample was placed in a Pt pan, kept at 298 K before the measurement, and then was heated under air at a rate of 10 K min^{-1}. Weight loss was estimated from the first differential of the TGA curve.

X-ray photoelectron spectroscopy: X-ray photoelectron spectroscopy (XPS) was measured using an X-ray photoelectron spectrometer (ESCALAB 200i-XL, Thermo Fisher Scientific Co. Ltd.) at a base pressure of 1×10^{-6} Pa. The X-ray source and power were Al K_α (1486.6 eV) and 200 W, respectively. Narrow multiplex scans were recorded with a 20 eV pass energy and 0.05 eV step size. Samples were ground with a mortar and pestle, and 10 mg of the sample was pressed (2 MPa) into a pellet disk that was attached to a cell holder with carbon tape. The background of each spectrum was subtracted by the Shirley method using Origin software (ver. 8). Binding energies were referenced to that of C 1s (284.5 eV).[2] The corrected spectra were normalized by the peak area of the C 1s XPS spectrum (peak areas were estimated by integrating the C 1s XPS spectrum).

Transmission electron microscopy: Transmission electron microscopy images were taken using two transmission electron microscopes (JEM-2100F/HK and JEM-ARM 200F, JEOL; accelerating voltage of 200 kV, High Voltage Electron Microscope Laboratory, Institute of Materials and Systems for Sustainability, Nagoya University, Japan). Samples were directly deposited on a Cu microgrid and blown with an air duster to remove excess material. The secondary-electron image (SEI) / annular dark-field (ADF) scanning transmission electron microscopy (STEM) and low-angle annular dark-field (LAADF) scanning transmission electron microscopy (STEM) images in Fig. 2 were measured by a transmission electron microscope (JEM-ARM200F, JEOL) in STEM mode.

Scanning electron microscopy: Scanning electron microscopy (SEM) images were taken using a scanning electron microscope (JSM-6700F, JEOL, Institute for Molecular Science, Japan). Two sets of parameters were used: (1) an accelerating voltage of 10 kV and magnification of 100,000 to 150,000×; and (2) an accelerating voltage of 5.0 kV and magnification of 300,000×. Samples were dispersed on carbon tape.

Pt L_{III}-edge X-ray absorption fine structure: X-ray absorption fine structure (XAFS) spectra at the Pt L_{III}-edge were measured in transmission mode at the BL9C and BL12C stations of the Photon Factory at KEK-IMSS (Tsukuba, Japan), and at the BL36XU station of SPring-8 (Hyogo, Japan). At the Photon Factory, the

energy and current of electrons in the storage ring were 2.5 GeV and 450 mA, respectively. X-rays from the storage ring were monochromatized using a Si(111) double-crystal monochromator, and ionization chambers filled with pure N_2 and N_2/Ar (85/15) gases were used to monitor the incident and transmitted X-rays, respectively. At SPring-8, the energy and current of the electrons in the storage ring were 8 GeV and 100 mA, respectively. X-rays from the storage ring were monochromatized using a Si(111) double-crystal monochromator, and ionization chambers filled with pure N_2 and Ar gases were used to monitor the incident and transmitted X-rays, respectively. All samples were measured at 20 K under vacuum.

Pt L_{III}-edge XAFS spectra were analyzed by ATHENA[3] and ARTEMIS[3] using IFEFFIT (ver. 1.2.11).[3] Threshold energy was tentatively set at the inflection point of the Pt L_{III}-edge (11 559 eV),[4] and the background was subtracted by the Autobk method.[5] The k^3-weighted extended XAFS (EXAFS) oscillations were Fourier transformed into *R*-space, and single-scattering curve-fitting analysis was performed in *R*-space. The fitting parameters for each shell were the coordination number (CN), interatomic distance (*R*), Debye-Waller factor (σ^2: mean square displacement), and correction-of-edge energy (ΔE_0). The value of S_0^2 was estimated by the EXAFS curve-fitting of Pt foil, and was fixed as 1 throughout the EXAFS analyses.

The curve-fitting analysis of **1** was conducted using one Pt–Pt and two Pt–O shells in *R*-space. ΔE_0 and σ^2 of two Pt–O bonds were fixed as the same values. Phase shifts and backscattering amplitudes were calculated with FEFF8 code[6] using the crystal structures of $Pt_4(\mu\text{-}OCOCH_3)_4(\mu\text{-}OCOC_2H_3)_4$.[7] The curve-fitting analyses of **A**, **pre-A**, and **A-noPPy** were conducted using Pt–Pt and Pt–O in *R*-space. Phase shifts and backscattering amplitudes were calculated with FEFF8 code[6] using the crystal structures of $Pt_4(\mu\text{-}OCOCH_3)_4(\mu\text{-}OCOC_2H_3)_4$[7] or Pt metal[8] for Pt–O and Pt–Pt.

Mechanism of Pt nanoparticle formation

Monitoring complex structure decomposition of 1 during co-polymerization: A solution of sodium dodecyl sulfonate (SDS) (40 mg) in distilled water (20 mL) was cooled to 274.5 K and kept at that temperature for 0.5 h. Pyrrole (98.0%, 0.025 mL, 0.36 mmol) was added dropwise to the solution, and a solution of **1** (16.4 mg, 11.3 μmol) in acetonitrile (1.6 mL) was then added. A solution of ammonium peroxydisulfate (APS) (4.01 mg, 17.6 μmol) in water (12 mL) was added dropwise at 274.5 K. The suspension was stirred at 274.5 K, and 80 μL of solution was collected at appropriate intervals. Each solution sample was diluted with acetonitrile to 5 mL using a volumetric flask and the UV/vis spectrum was measured using a V-550 spectrometer (JASCO).

Measurement of electrocatalytic performance

Electrochemical measurements: Electrochemical measurements were performed on an electrochemical analyzer (760D, ALS) using a three-electrode cell in 0.1 M aqueous perchloric acid ($HClO_4$) solution (70%, 99.999% trace metal basis, Sigma-Aldrich) at 293 K. A Pt sheet and reversible hydrogen electrode (RHE) were used as the counter and reference electrodes, respectively. Cyclic voltammetry was carried out in the potential range of 0.1–1.2 V_{RHE} at a scanning rate of 50 mV s^{-1} in N_2 (99.9999%)-saturated 0.1 M $HClO_4$ solution. The electrochemical surface area (ECSA) of Pt in the catalysts was calculated by

$$\mathrm{ECSA} = \frac{\mathrm{Q_H}}{2.1\,\mathrm{C\,m^{-2}} \times \mathrm{L_{Pt}}}$$

where Q_H (mC) is the average charge transfer for the hydrogen adsorption and desorption of the cyclic voltammograms (0.05–0.4 V_{RHE}), 2.1 C m^{-2} is the electrical charge for monolayer adsorption of hydrogen on a Pt nanocrystal surface, and L_{Pt} (g) is the Pt loading on the working electrode.

ORR activities of the catalysts were measured by linear sweep voltammetry in the potential range of 0.05–1.0 V_{RHE} at a scanning rate of 10 mV s^{-1} in O_2 (99.9999%)-saturated 0.1 M $HClO_4$ solution through the RDE method (rotation rates of 400, 900, 1600, and 2500 rpm). The background current was measured in the potential range of 0.05–1.0 V_{RHE} at a scanning rate of 10 mV s^{-1} in N_2-saturated 0.1 M $HClO_4$ solution. The ORR data were corrected by ohmic *i*R drop compensation and background currents. Koutecký-Levich plots were collected at 0.9 V_{RHE} for all measured catalysts. The intercept of the best linear fit lines of the Koutecký-Levich plots was used to analyze the kinetic current density (j_k) involved in the typical ORR process based on the Koutecký-Levich equation,

$$\frac{1}{j} = \frac{1}{j_{\mathrm{k}}} + \frac{1}{j_{\mathrm{L}}} = \frac{1}{j_{\mathrm{k}}} + \frac{1}{B\omega^{1/2}}$$

$$B = 0.62nFC_0\left(D_0\right)^{2/3}\nu^{-1/6}$$

where j is the measured current density, j_L is the diffusion-limiting current density, ω is the angular velocity, n is the transferred electron number, F is the Faraday constant, C_0 is the bulk concentration of O_2, D_0 is the diffusion coefficient of O_2 in the electrolyte, and ν is the kinetic viscosity of the electrolyte. Mass-specific activity (MSA) and surface specific activity (SSA) were calculated by normalizing the kinetic current to ECSA and Pt loading.

The accelerated degradation test (ADT) was carried out up to 30 000 repeated potential step cycles (1.0 V_{RHE}, 3 s to 0.6 V_{RHE}, 3 s, 6000 cycles/one unit) in N_2-saturated 0.1 M $HClO_4$ solution after keeping the initial potential at 0.6 V_{RHE} for 2 sec.

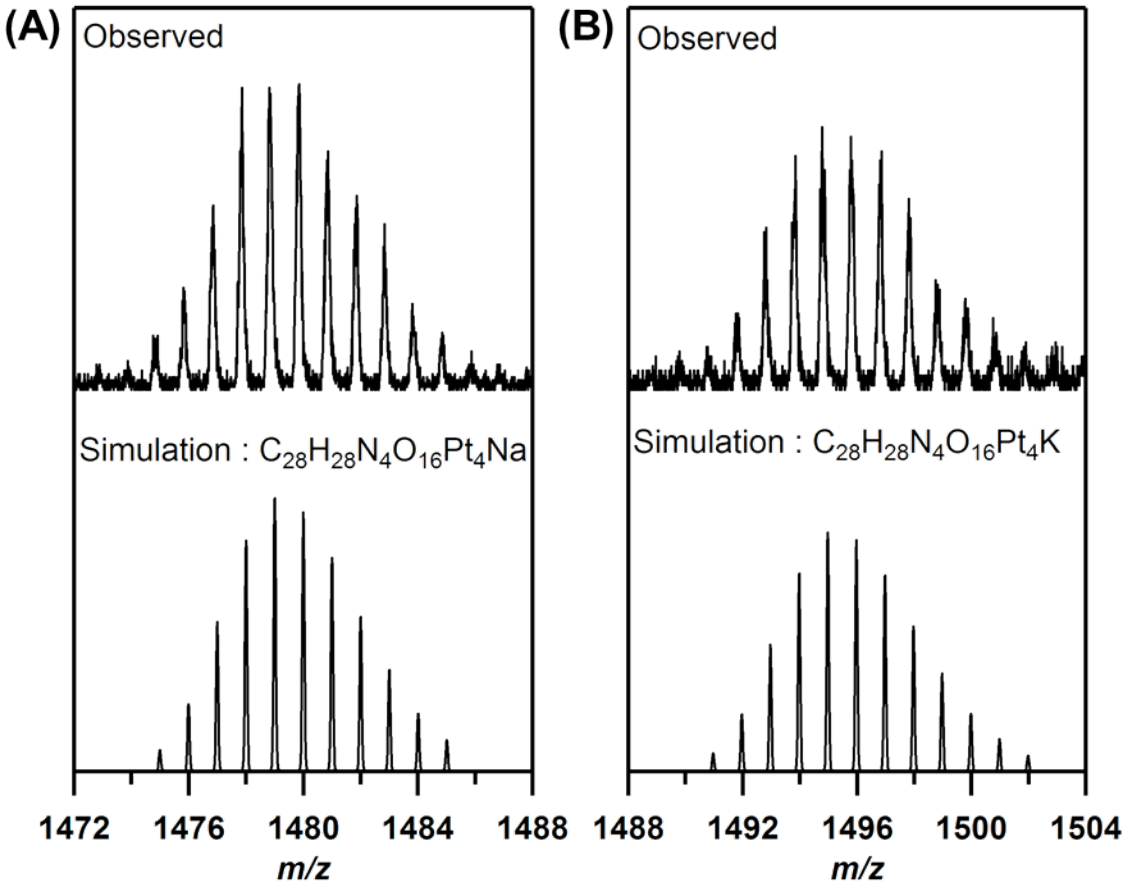

Fig. I. Observed and simulated ESI-MS spectra of (A) [**1** + Na]$^+$ and (B) [**1** + K]$^+$.

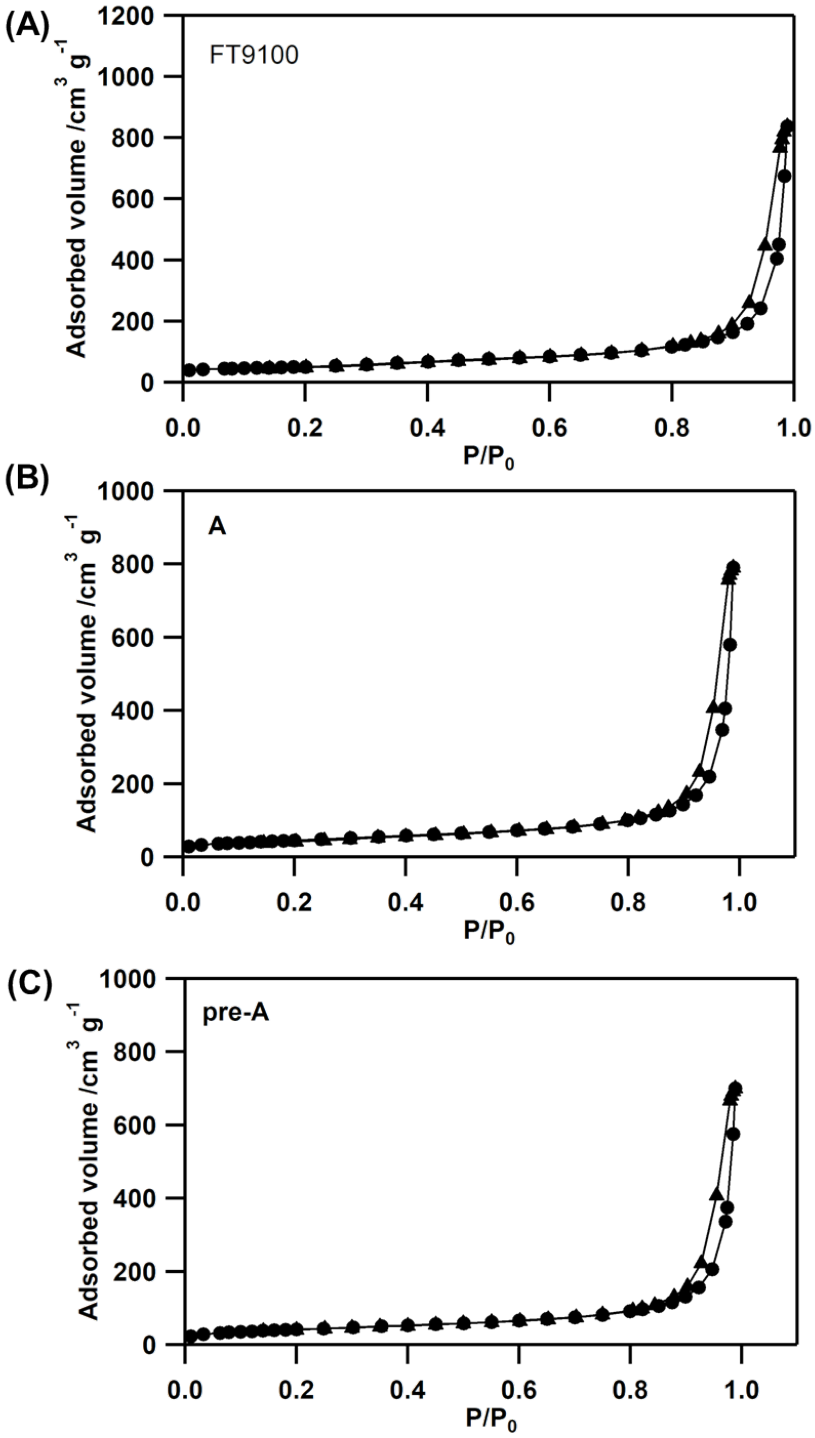

Fig. S1. Nitrogen adsorption isotherms at 77 K for (A) FT9100, (B) **A**, and (C) **pre-A**. Solid and dotted lines show adsorption (●) and desorption (▲) of nitrogen, respectively.

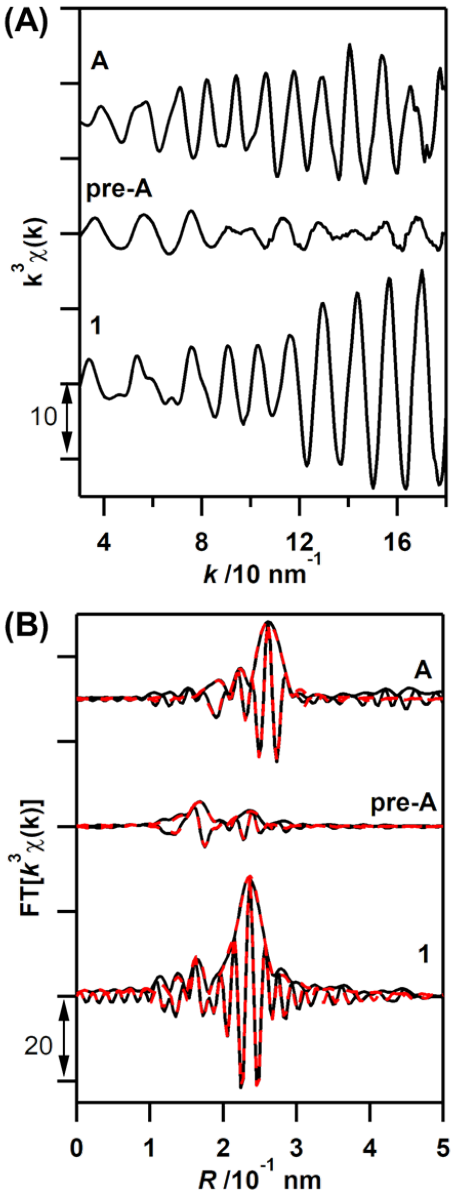

Fig. S2. (A) k^3-Weighed Pt L_{III}-edge EXAFS oscillations and (B) their Fourier transforms (k = 30–180 nm^{-1}) for **1**, **A**, and **pre-A** measured at 20 K. Black solid lines in (B) show observed data and red dashed lines show fitted data.

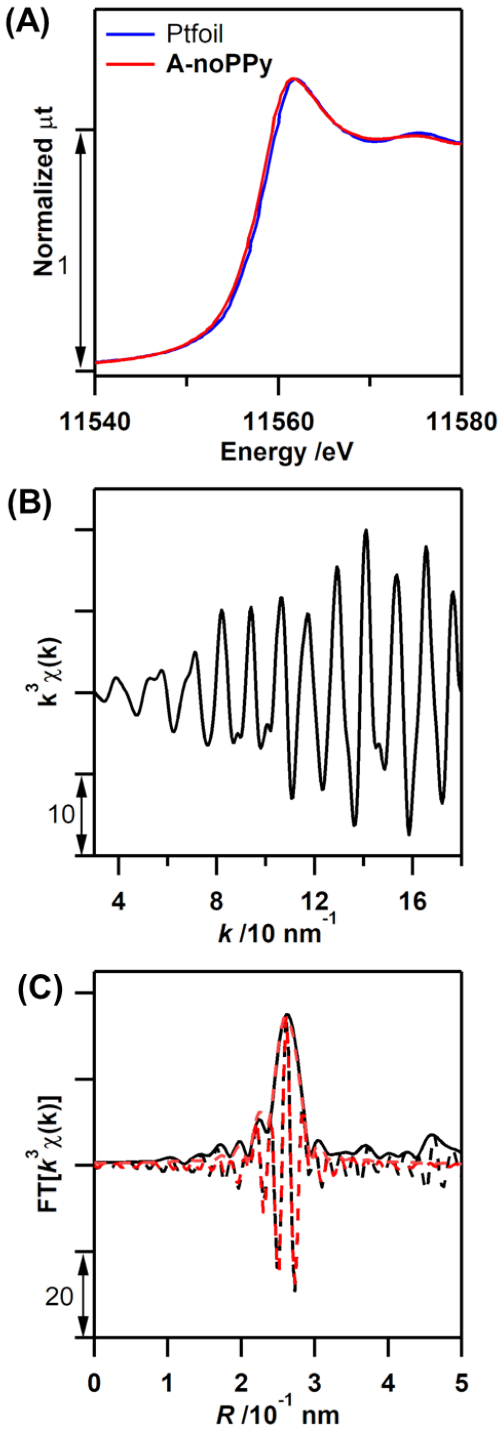

Fig. S3. (A) Normalized Pt L_{III}-edge XANES, (B) k^3-weighed Pt L_{III}-edge EXAFS oscillations, and (C) their Fourier transforms (k = 30–180 nm^{-1}) for **A-noPPy** measured at 20 K. Black solid lines in (C) show observed data and red dashed lines show fitted data.

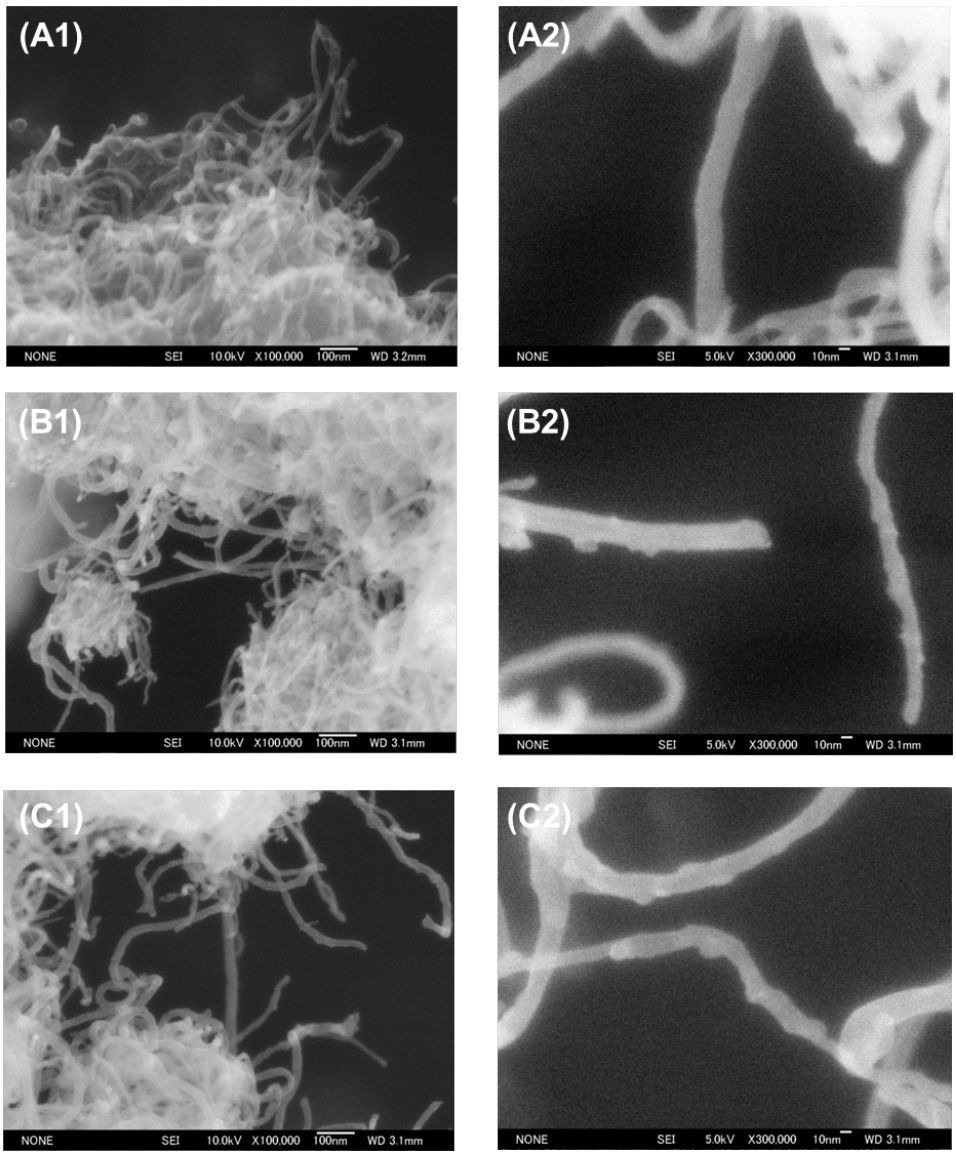

Fig. S4. SEM micrographs of (A) FT9110, (B) **A**, and (C) **pre-A**.

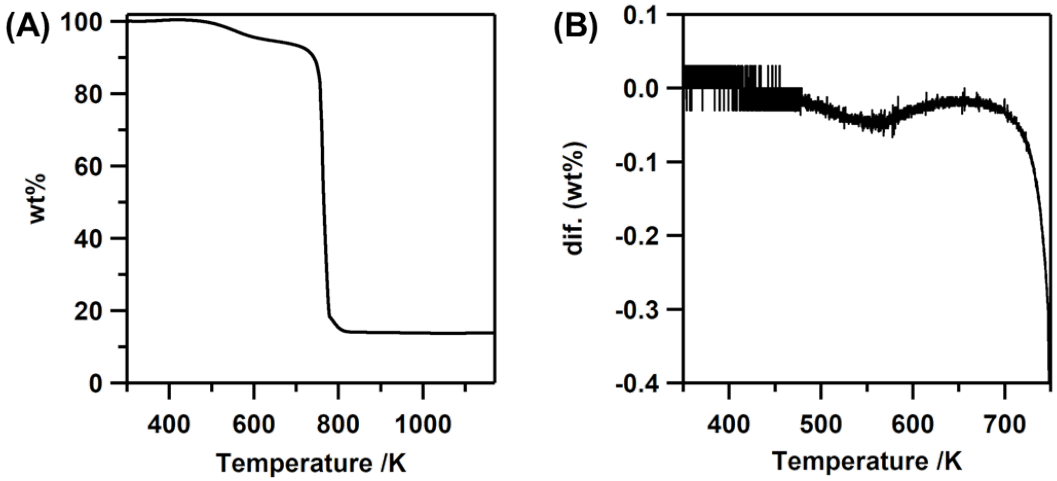

Fig. S5. (A) TGA curve of **A** and (B) TGA differential plot of **A**.

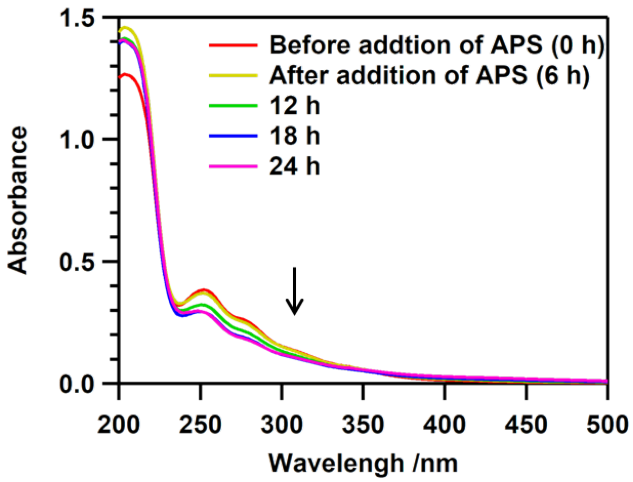

Fig. S6. UV/vis spectra of a mixed solution of **1**, pyrrole, and SDS in water/acetonitrile after the addition of APS.

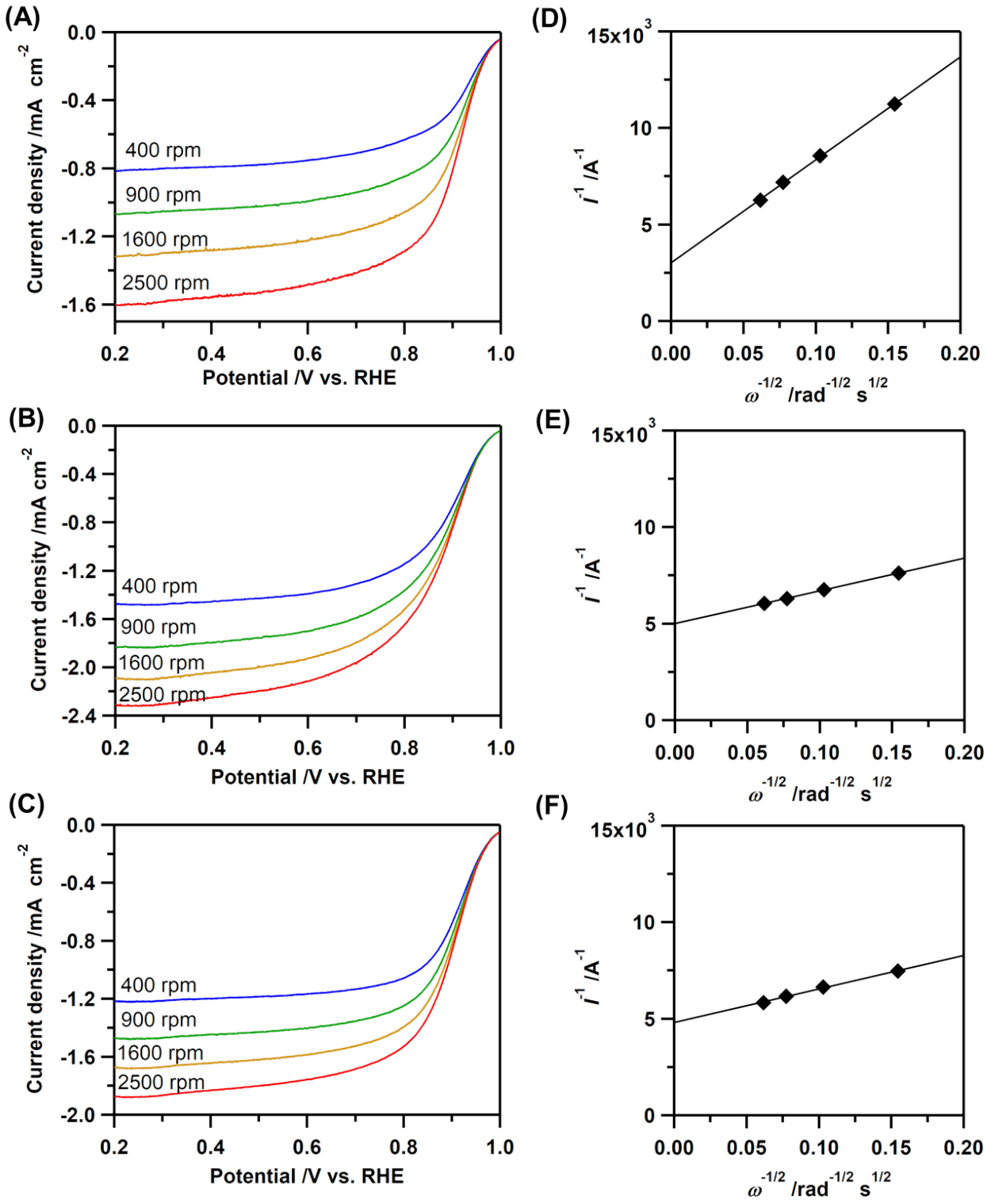

Fig. S7. (A) (B) (C) Linear sweep voltammograms of (A) **A**, (B) **A-noPPy**, and (C) TEC10E50E at different rotation speeds (400, 900, 1600, and 2500 rpm) before ADT recorded at a scanning rate of 10 mV s^{-1} in O_2-saturated 0.1 M $HClO_4$ solution. (D) (E) (F) Koutecký-Levich plots of (D) **A**, (E) **A-noPPy**, and (F) TEC10E50E obtained from linear sweep voltammopgrams at diffetent rotation rates (400, 900, 1600, and 2500 rpm) at 0.9 V (vs RHE) recorded at a scanning rate of 10 mV s^{-1} in O_2-saturated 0.1 M $HClO_4$ solution.

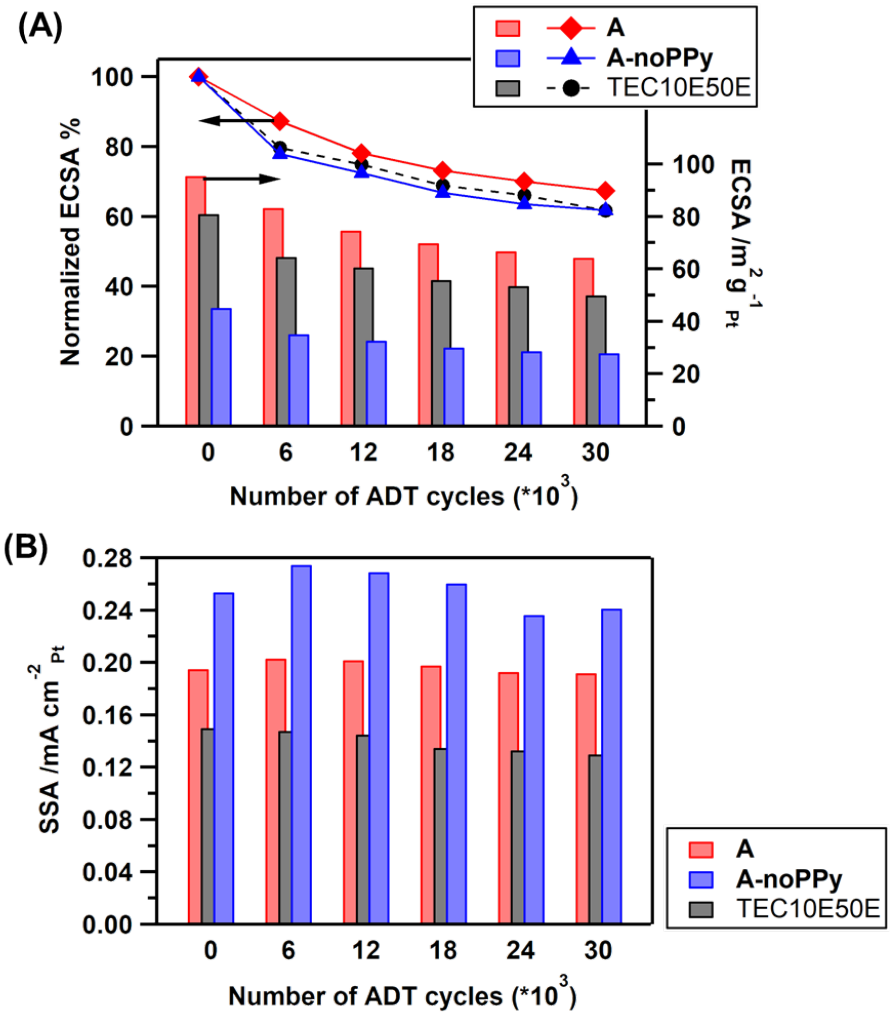

Fig. S8. (A) ECSA and (B) SSA of **A** (red), **A-noPPy** (blue), and TEC10E50E (black) at 0.9 V before and after ADT at different cycles (6000, 12 000, 18 000, 24 000, and 30 000 cycles).

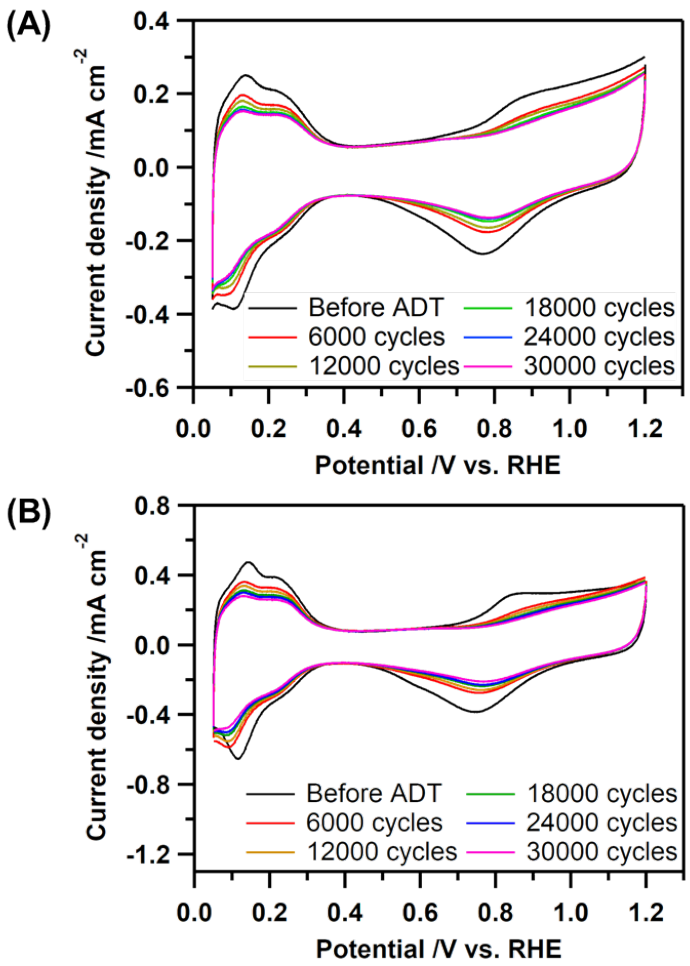

Fig. S9. Cyclic voltammograms of (A) **A-noPPy** and (B) TEC10E50E after ADT for 6000, 12 000, 18 000, 24 000, and 30 000 cycles, recorded at a scanning rate of 50 mV s^{-1} in N_2-saturated 0.1 M $HClO_4$ solution.

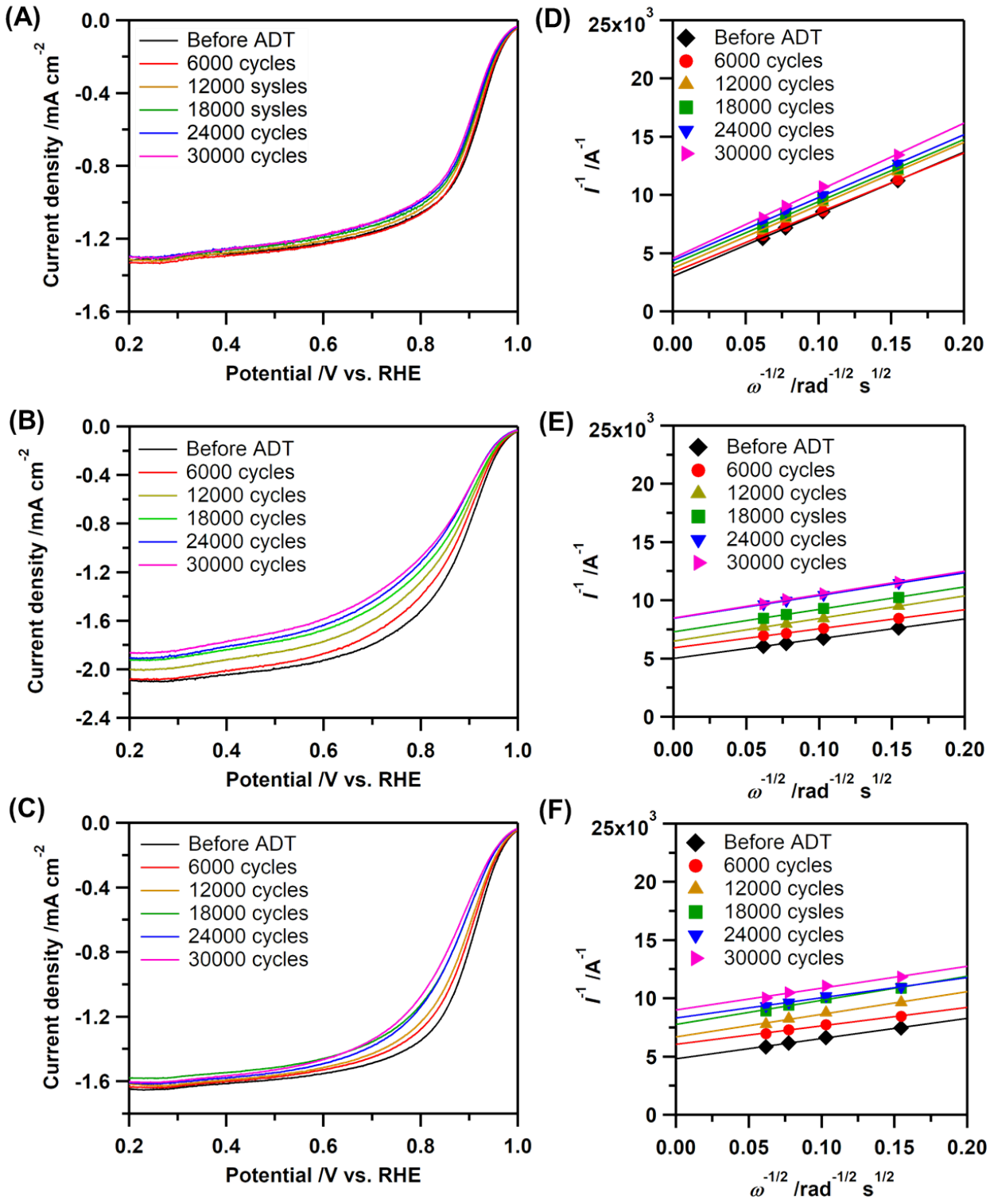

Fig. S10. (A) (B) (C) Linear sweep voltammograms of (A) **A**, (B) **A-noPPy**, and (C) TEC10E50E (1600 rpm) before and after ADT at different cycles (6000, 12 000, 18 000, 24 000, and 30 000 cycles) recorded at a scanning rate of 10 mV s^{-1} in O_2-saturated 0.1 M $HClO_4$ solution. (D) (E) (F) Koutecký-Levich plots of (D) **A**, (E) **A-noPPy**, and (F) TEC10E50E obtained from linear sweep voltammopgrams at diffetent rotation rates (400, 900, 1600, and 2500 rpm) at 0.9 V (vs RHE) before and after ADT at different cycles (6000, 12 000, 18 000, 24 000, and 30 000 cycles) recorded at a scanning rate of 10 mV s^{-1} in O_2-saturated 0.1 M $HClO_4$ solution.

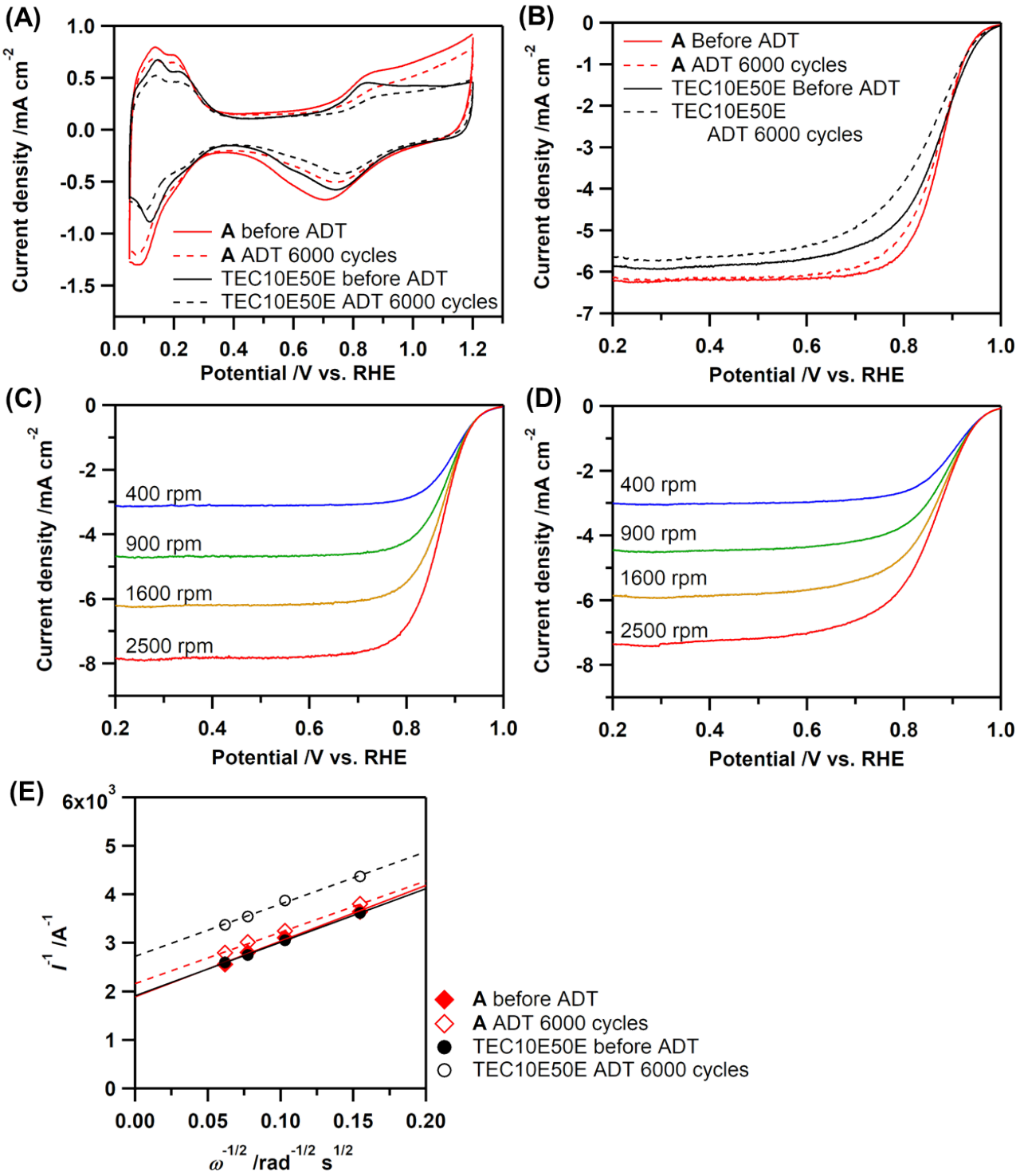

Fig. S11. Electrocatalytic data for ORR with catalysts prepared under optimum conditions. (A) Cyclic voltammograms of **A** and TEC10E50E before and after ADT at 6000 cycles recorded at a scanning rate of 50 mV s^{-1} in N_2-saturated 0.1 M $HClO_4$ solution. (B) Linear sweep voltammograms of **A** and TEC10E50E (1600 rpm) before and after ADT at 6000 cycles recorded at a scanning rate of 10 mV s^{-1} in O_2-saturated 0.1 M $HClO_4$ solution. (C) (D) Linear sweep voltammograms of (C) **A** and (D) TEC10E50E at different rotation speeds (400, 900, 1600, and 2500 rpm) before ADT recorded at a scanning rate of 10 mV s^{-1} in O_2-saturated 0.1 M $HClO_4$ solution. (E) Koutecký-Levich plots of **A** and TEC10E50E obtained from linear sweep voltammopgrams at different rotation rates (400, 900, 1600, and 2500 rpm) at 0.9 V (vs RHE) before and after ADT at 6000 cycles. (F) (G) (H) Change in (F) ECSA, (G) MSA, and (H) SSA of **A** (red) and TEC10E50E (black) at 0.9 V before and after ADT at 6000 cycles.

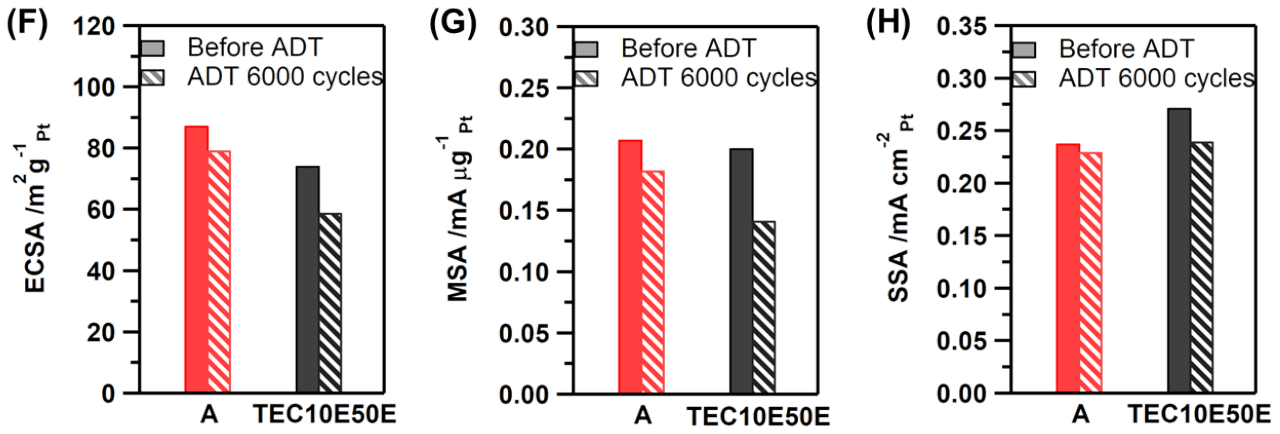

Fig. S11 (Continued). Electrocatalytic data for ORR with catalysts prepared under optimum conditions. (A) Cyclic voltammograms of **A** and TEC10E50E before and after ADT at 6000 cycles recorded at a scanning rate of 50 mV s^{-1} in N_2-saturated 0.1 M $HClO_4$ solution. (B) Linear sweep voltammograms of **A** and TEC10E50E (1600 rpm) before and after ADT at 6000 cycles recorded at a scanning rate of 10 mV s^{-1} in O_2-saturated 0.1 M $HClO_4$ solution. (C) (D) Linear sweep voltammograms of (C) **A** and (D) TEC10E50E at different rotation speeds (400, 900, 1600, and 2500 rpm) before ADT recorded at a scanning rate of 10 mV s^{-1} in O_2-saturated 0.1 M $HClO_4$ solution. (E) Koutecký-Levich plots of **A** and TEC10E50E obtained from linear sweep voltammopgrams at different rotation rates (400, 900, 1600, and 2500 rpm) at 0.9 V (vs RHE) before and after ADT at 6000 cycles. (F) (G) (H) Change in (F) ECSA, (G) MSA, and (H) SSA of **A** (red) and TEC10E50E (black) at 0.9 V before and after ADT at 6000 cycles.

Table S1. Structural Parameters Obtained by Curve-fitting Analysis of Pt L_{III}-edge EXAFS Measured at 20 K[a]

Shell	CN	R / nm	ΔE_0	σ^2 / 10^5 nm^2
		$C_{20}H_{24}O_{16}Pt_4$ (X-ray single crystal)[b]		
Pt–Pt	2	0.249	---	---
Pt–O	2	0.191	---	---
Pt–O	2	0.214	---	---
		1[c]		
Pt–Pt	2.3 ± 0.3	0.250 ± 0.001	8 ± 3	2 ± 1
Pt–O	2.3 ± 0.6	0.203 ± 0.002	8 ± 4	2 ± 1
Pt–O	1.6 ± 0.6	0.219 ± 0.002	8 ± 4	2 ± 1
		pre-A[d]		
Pt–Pt	0.6 ± 0.3	0.251 ± 0.001	-6 ± 6	4 ± 1
Pt–O	1.9 ± 0.3	0.200 ± 0.001	16 ± 2	4 ± 1
		A[e]		
Pt–Pt	5.4 ± 1.0	0.276 ± 0.001	11 ± 2	5 ± 1
Pt–O	0.8 ± 0.4	0.216 ± 0.002	19 ± 5	1 ± 1
		A-noPPy[f]		
Pt–Pt	7.3 ± 0.7	0.277 ± 0.001	12 ± 1	4 ± 1

[a] S_0^2 was fixed to be 1. k = 30–180 nm^{-1}. [b] Ref. 7. [c] R = 0.12–0.30 nm, R_f = 0.6%. [d] R = 0.12–0.26 nm, R_f = 2.2%. [e] R = 0.13–0.32 nm, R_f = 1.3%. [f] R = 0.18–0.32 nm, R_f = 0.8%.

References

1. T. Yamaguchi, Y. Sasaki, A. Nagasawa, T. Ito, N. Koga, K. Morokuma, *Inorg. Chem*. 1989, **28**, 4312−4314.

2. T. I. T. Okpalugo, P. Papakonstantinou, H. Murphy, J. McLaughlin, N. M. D. Brown, *Carbon* 2005, **43**, 153−161.

3. (a) B. Ravel, M. Newville, *J. Synchrotron Radiat*. 2005, **12**, 537−541. (b) M. Newville, B. Ravel, D. Haskel, J. J. Rehr, E. A. Stern, Y. Yacoby, *Physica B* 1995, **208-209**, 154−156.

4. J. A. Bearden, A. F. Burr, *Rev. Mod. Phys.* 1967, **39**, 125−142.

5. (a) M. Newville, *J. Synchrotron Rad*. 2001, **8**, 322−324. (b) M. Newville, P. Līviņŝ, Y. Yacoby, J. J. Rehr, E. A. Stern, *Phys. Rev. B* 1993, **47**, 14126−14131.

6. A. L. Ankudinov, B. Ravel, J. J. Rehr, S. D. Conradson, *Phys. Rev. B* 1998, **58**, 7565−7576.

7. M. Ohashi, A. Yagyu, Q. Xu, K. Mashima, *Chem. Lett*. 2006, **35**, 954−955.

8. W. P. Davey, *Phys. Rev*. 1925, **25**, 753−761.